MODELING OF MICROBAROM SIGNALS IN THE PACIFIC

Milton Garcés, Claus Hetzer, Steven Businger, and Mark Willis

University of Hawaii, Manoa

Sponsored by Defense Threat Reduction Agency

Contract No. DTRA01-01-C-0077

ABSTRACT

Severe weather in the ocean generates infrasonic signals in the 0.1- to 0.5-Hz frequency band that can propagate for thousands of kilometers. The source generation mechanism for microbaroms is believed to be the same as for microseisms, and is attributed to the nonlinear interaction of surface ocean waves. We compare theoretical predictions with infrasonic observations of Hurricane Daniel in July of 2000. The nonlinear interaction of the ocean wave field is predicted to radiate sound waves only if the ocean waves are almost opposite in direction and of a near identical frequency. However, perfectly opposing wave trains of the same frequency radiate vertically, and this acoustic energy never returns back to the earth. Only opposing wave trains that are slightly off line or with slightly different frequencies will result in isotropic acoustic radiation, even for highly directional ocean wave fields. The slowness of the infrasonic waves observed by International Monitoring System (IMS) array IS59, or KONA, suggests that these waves were propagating close to the horizontal. The observed azimuth of the incident sound waves corresponds to the most energetic stage of Daniel's lifespan, and suggests that the acoustic signals were radiated during the interaction of surface gravity waves in the open ocean. Using the known dispersion relation for deep water waves, the median detection frequency corresponds to ocean wave speeds that are slower than the known hurricane track speed of Daniel, a condition that would encourage the nonlinear interaction.

OBJECTIVE

The aim of this work is to characterize microbarom signals observed in the Pacific and model the source processes that generate these signals, with the aim of determining infrasonic detection thresholds in the microbarom frequency range.

RESEARCH ACCOMPLISHED

1. Introduction

Infrasonic signals known as microbaroms consist of pressure oscillations with dominant periods of 4-7 s, and they can appear as energy bursts or as a continuous oscillation that can last for hours or days. In the frequency domain, microbaroms appear as a broad frequency peak centered around 0.2-0.3 Hz (Figure 1). Like microseisms in seismology (Kibblewhite and Wu, 1996), microbaroms are thought to be generated by the nonlinear interaction of ocean surface waves. For infrasonic stations near the ocean, microbaroms determine the noise floor in the 0.1-0.5 Hz frequency band, and thus determines the detection thresholds in that band. In Hawaii, microbarom signals are determined from all azimuths (Garces and Hetzer, 2002), and the dominant signal is usually corresponds to either the closest storm to the recording station or the largest wave heights associated with severe weather in the Pacific.

2. Theoretical background

Our starting assumption is that the source generation mechanisms for microbaroms is similar to that of microseisms. However, microseisms and microbaroms will have very different propagation paths. Energy launched near a vertical angle to the ocean surface and towards the ocean floor couples well with the bedrock, and energy launched just below the ocean surface may not reach the ground. In contrast, energy launched near a vertical angle into the atmosphere never returns back to the Earth, and most of the infrasonic signals recorded by ground stations correspond to energy launched near the horizontal angle at the source. The radiation pattern of microbarom sources is discussed below.

For a specified ocean surface wave velocity u_z, the far-field acoustic pressure, p, in a homogeneous atmosphere can be expressed as (Arendt and Fritz, 2000),

$$p\left(x, y, z, t - \frac{R}{c}\right) = -\frac{\rho_0}{8\pi c}\frac{\partial}{\partial t}\int \frac{z}{R^2} u_z^2 \, dx' \, dy'$$

$$R^2 = (x - x')^2 + (y - y')^2 + z^2$$

where x,y, and z are the spatial coordinates in a Cartesian reference frame, x' and y' are the Cartesian coordinates of integration over the ocean surface, ρ_o is the atmospheric density, and c is the atmospheric sound speed. Note that the acoustic pressure is proportional to the integral of the square of the ocean surface velocity. After expressing the ocean surface velocity as sinusoidal terms corresponding to propagating surface wave trains, we find propagating acoustic solutions only exist for surface waves that interact with each other at near the same frequency and nearly anti-parallel directions. All other solutions are non-propagating.

The period and amplitude of an ocean wave depend on the wind speed and fetch of a severe weather disturbance. Although high wind speeds are possible in a hurricane, such winds are usually highly localized, have a relatively small fetch, and thus do not efficiently generate large ocean waves. Ocean surface waves that propagate for long ranges usually have periods of 8-12 seconds. Due to the nonlinear interaction introduced by the square of the velocity, the acoustic solution will have approximately twice the ocean wave frequency (frequency doubling). This can be understood as an acoustic coupling, as for sound to be efficiently radiated in the atmosphere it is necessary for the horizontal wavelength of the ocean wave field to match the acoustic wavelength. Due to the slow propagation speed of deep water waves, their wavelength tends to be too small for acoustic coupling unless two surface wave trains are propagating nearly opposite to each other, in which case one of the nonlinear terms allows the existence of a large horizontal wavelength (small horizontal wave number) that encourages efficient coupling to the atmosphere. This nonlinear term corresponds to an acoustic frequency that is the sum of the frequencies of the interacting surface wave trains, or approximately twice the dominant frequency of the ocean wave. Figure 2 shows the real part of the vertical component of the acoustic wave number as a function of ocean surface wave number (upper panel) and acoustic wave number (lower panel).

The wave number solution space for the surface wave velocity corresponds to two waves propagating in almost parallel but opposite directions. However, the acoustic solution space is isotropic, which implies that even a very directional surface wave field can generate infrasonic waves along all azimuths. This isotropic acoustic radiation pattern helps explain the pervasiveness of the microbarom signals. When ocean waves propagate exactly against each other at the same frequency, the nonlinear interaction produces a piston-like displacement of the ocean surface, and launches sound straight up to the atmosphere. Maximum acoustic energy is radiated in the vertical direction, and although it may contribute to the atmosphere's heating (Rind, 1977), this energy is lost to space and cannot be recorded by ground-based stations. Infrasound arrays would only record microbarom signals that are launched close to the horizontal, corresponding to ocean waves interacting at slightly dissimilar frequencies and slightly off the anti-parallel directions. Thus, only a small fraction of the total acoustic energy launched into the atmosphere by microbarom sources reaches the ground.

3. Case study: Hurricane Daniel

Approximately two months after the initiation of operations of IMS array I59US in Hawaii, Hurricane Daniel formed in the eastern Pacific and steadily moved towards Hawaii. Figure 3 shows the track history of Daniel, and the arrival azimuth of infrasonic signals detected by I59US, also referred to as KONA. All microbarom detections were computed using the PMCC method described in Garces and Hetzer (2002). We see that infrasonic detection of Daniel started before it was designated a hurricane (Figure 3, red), and the detected azimuth matches the actual azimuth of Daniel up to August 1, when Daniel began to dissipate. Figure 4 shows the frequency content of the microbarom signals recorded by KONA. Most of the energy is in the 0.1-0.4 Hz band, and there is a bifurcation in the microbarom band from late July 30 to early August 1. The track speed and maximum wind speed of Daniel is shown in Figure 5. The frequency of the optimal detection at KONA and the range of Daniel from KONA is plotted in the upper panel of Figure 6. Using the dispersion relation for deep water ocean waves, the propagation group velocity for surface waves at the frequency of optimal detection is shown in the lower panel of Figure 6, superposed with the track velocity of Daniel. For a 10 s ocean wave period, the acoustic period will be 5 s, corresponding to a frequency of 0.2 Hz. The group velocity for a 10 s ocean wave is ~ 8m/s. As mentioned in the previous section, a prerequisite for acoustic radiation is the presence of surface waves interacting nearly anti-parallel to each other. Two scenarios in which this condition may be maintained involve (1) a storm system that is propagating faster than the group velocity of surface waves, and (2) surface waves reflected from continents or island. The lower panel of Figure 6 suggest that the initial source of microbarom generation involved the first mechanism, but the later detections involved both mechanisms. Reflections of the storm-generated ocean waves from the islands may also explain the frequency bifurcation in the spectral content of the signals, which correspond to the close proximity of Daniel after July 30.

CONCLUSIONS AND RECOMMENDATIONS

Initial work has been performed in the evaluation of the infrasonic field predicted from storm activity in the Pacific. The theoretical results are consistent with infrasonic observations of Hurricane Daniel as it approached Hawaii. Infrasound from Daniel appears to be initially generated by the interaction of ocean waves generated behind and ahead of the hurricane core as it moved faster than the propagation speed of the ocean waves. As Daniel approached Hawaii, some higher frequency infrasound may have been generated by the interaction of the direct ocean waves with reflections from the island chain. Further work is needed on quantifying the relationships between hurricane dynamics, surface ocean wave generation, and infrasound generation.

REFERENCES

Arendt, S., and D. Fritts (2000). Acoustic radiation by ocean surface waves. *J. Fluid Mech*, **415**, 1-21.

Garces, M., and C. Hetzer (2002). Evaluation of infrasonic detection algorithms. This volume.

Kibblewhite, A., and Cheng Y. Wu (1996). Wave interactions as a seismo-acoustic source. Lecture Notes in Earth Sciences, Springer-Verlag, Berlin.

Rind, D. (1977). Heating of the lower thermosphere by the dissipation of acoustic waves. *J. Atmospheric and Terrestrial Physics*, **39**, 445-456.

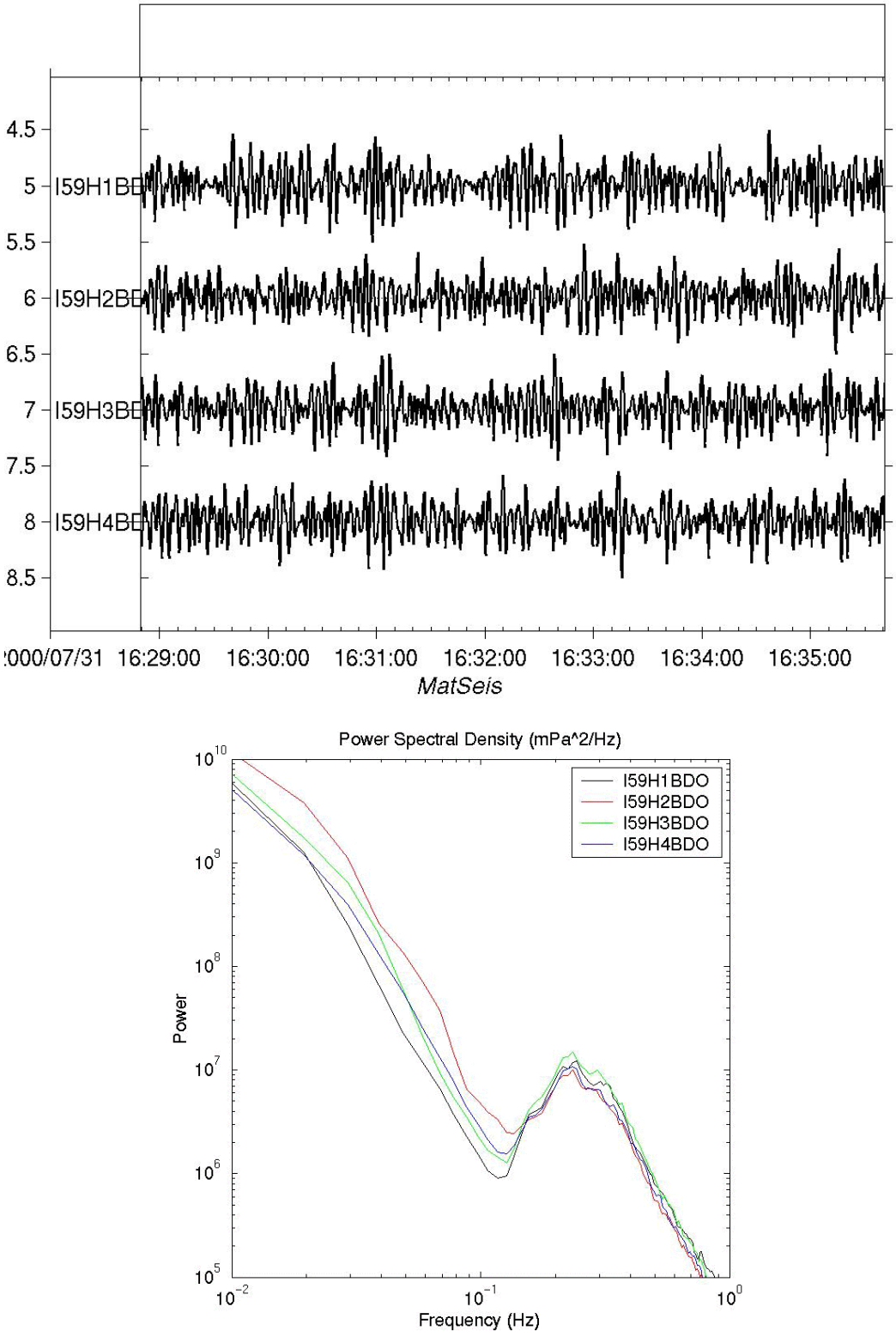

Figure 1. Example of microbarom signals recorded in Hawaii on July 31, 2000, and power spectral density for the same time period.

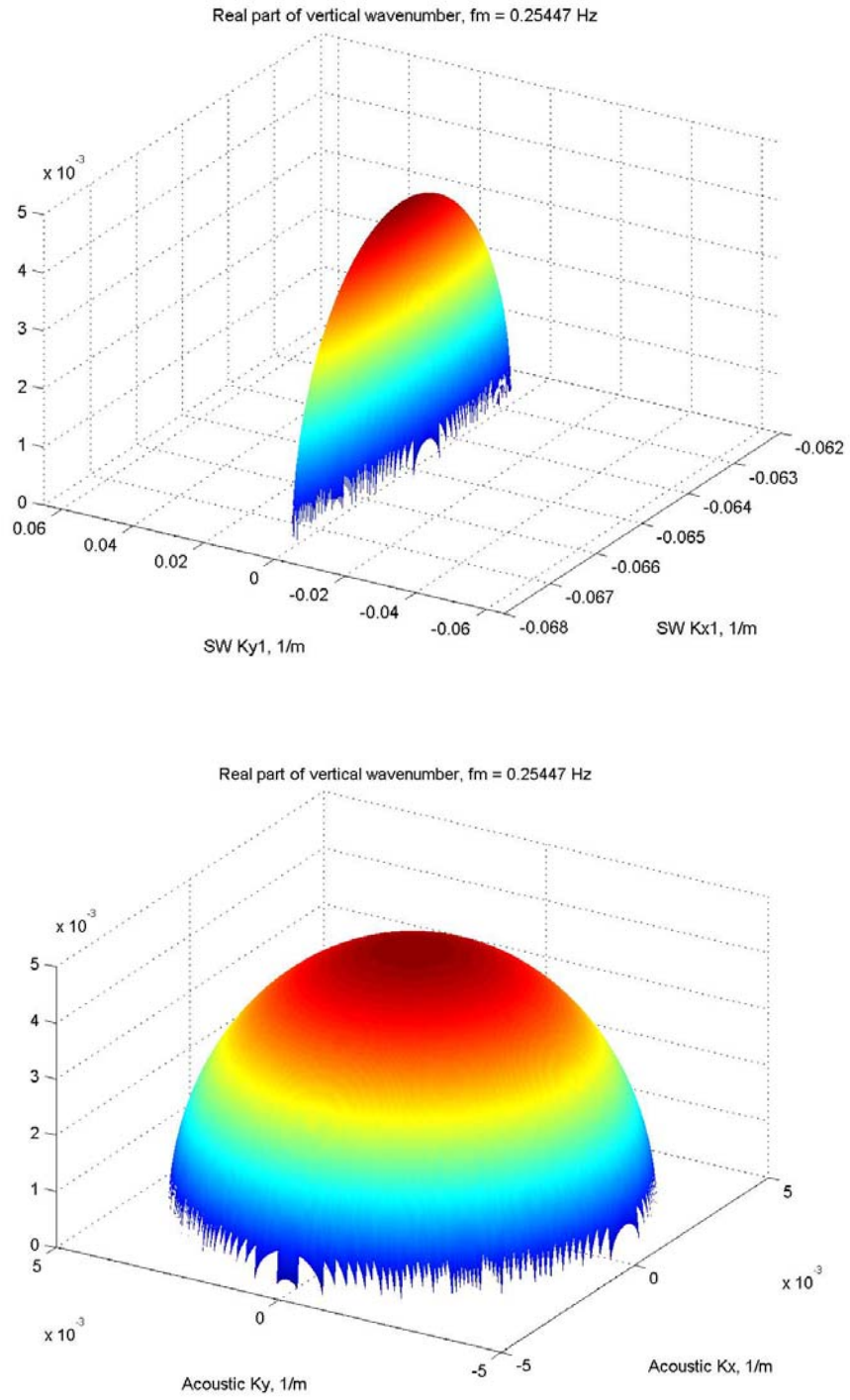

Figure 2. Real part of the vertical wave number of the acoustic solution of Arendt and Fritz (2000) for a surface wave period of ~8 s propagating along the horizontal direction (ky = 0, kx>0) and interacting with a second ocean wave of arbitrary direction. The upper panel shows the acoustic solution only exists for a small range of ocean wave numbers corresponding to the second surface wave propagating nearly anti-parallel (ky << kx, kx <0) to the first wave. The lower panel shows the real part of the acoustic vertical wave number as a function of the horizontal wave number, illustrating the isotropic nature of the acoustic radiation pattern.

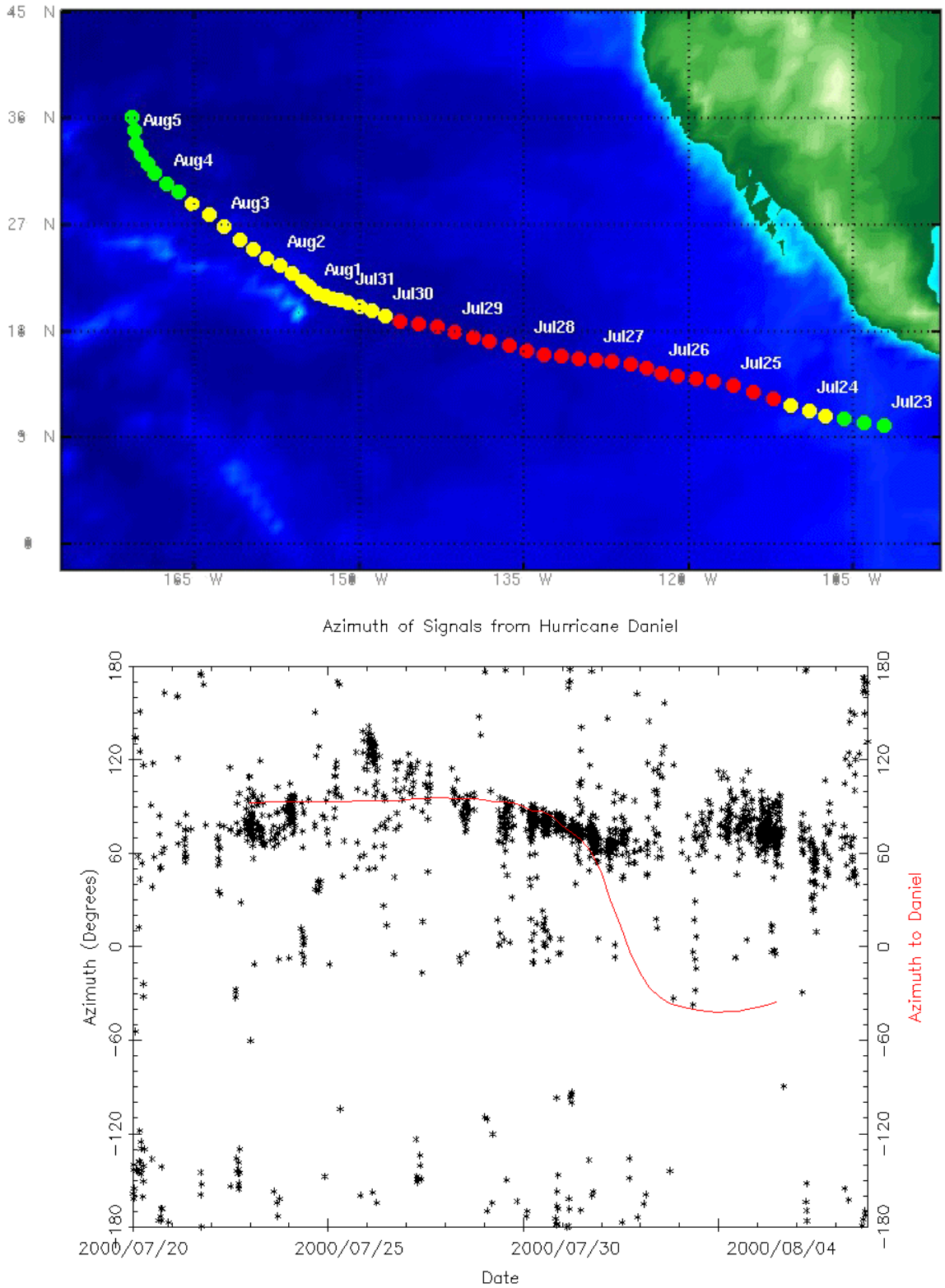

Figure 3. Track of Daniel (upper panel) and observed infrasonic arrival azimuth (lower panel), measured clockwise from N, for microbarom signals observed in KONA for the same period. The red line in the lower panel marks the azimuth from Hawaii to Daniel's core.

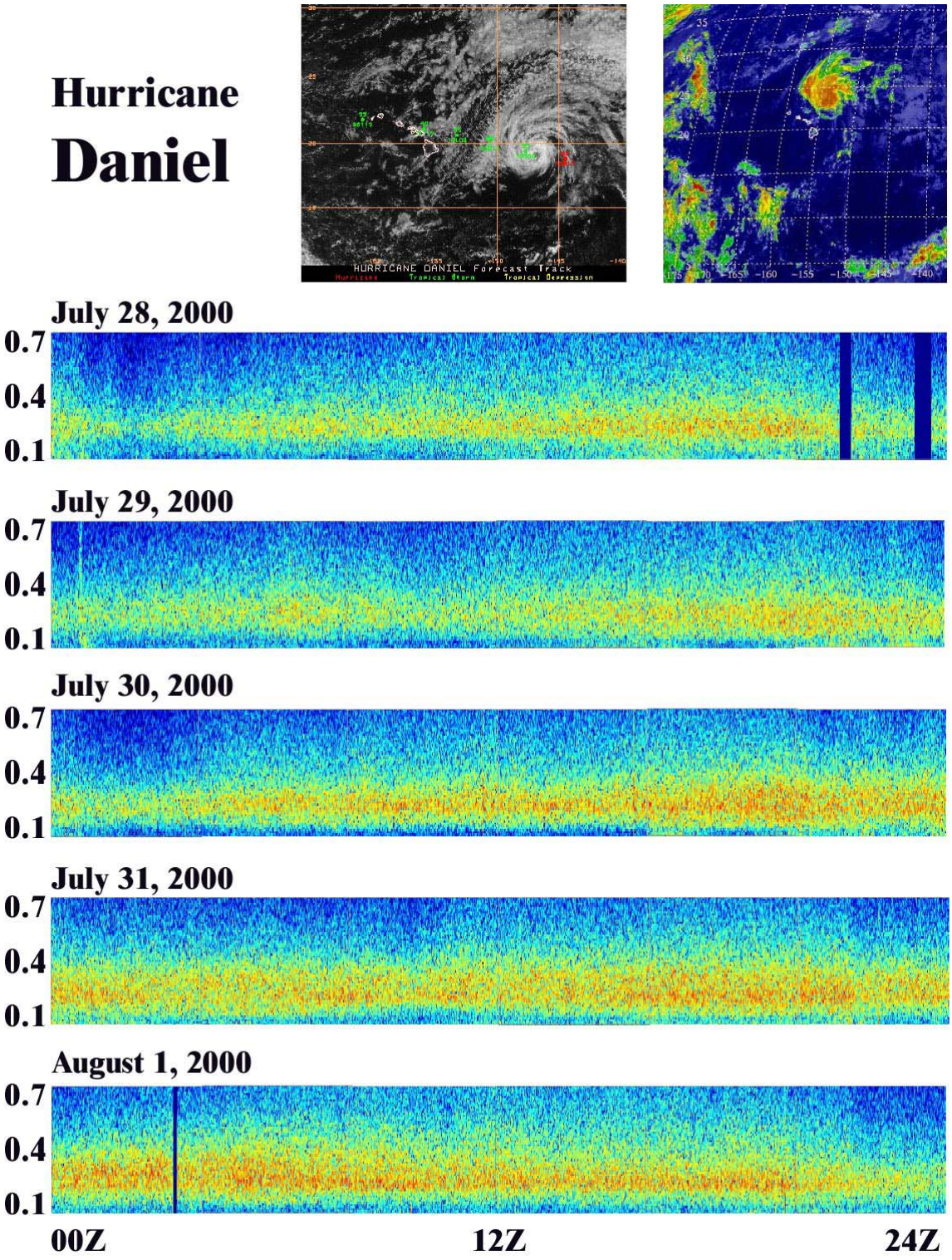

Figure 4. Spectrograms in the microbarom range for Daniel, showing initial diurnal fluctuations in the microbarom levels, which disappear as Daniel approached Hawaii. Note the frequency bifurcation starting after 12Z on July 30 and ending around 12Z on August 1.

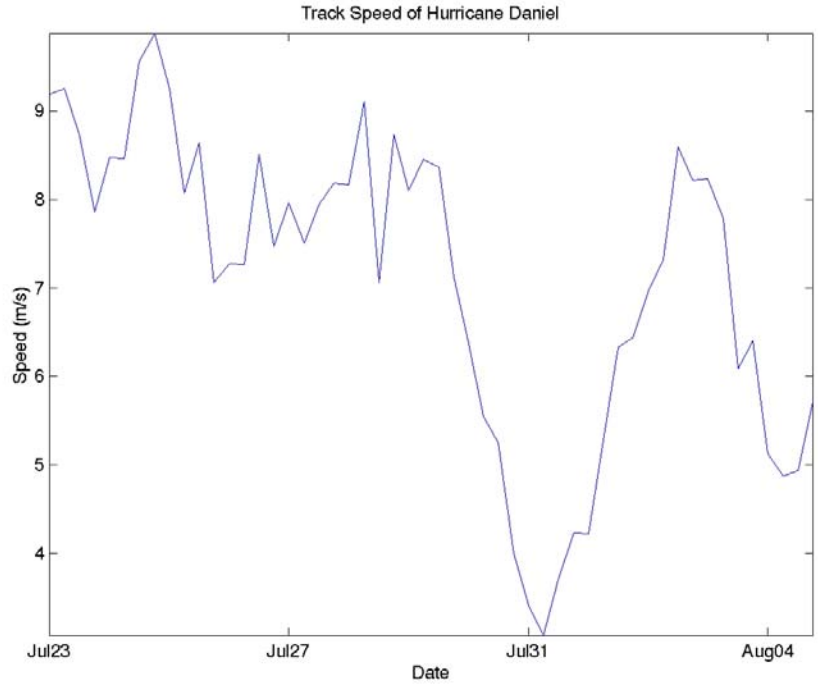

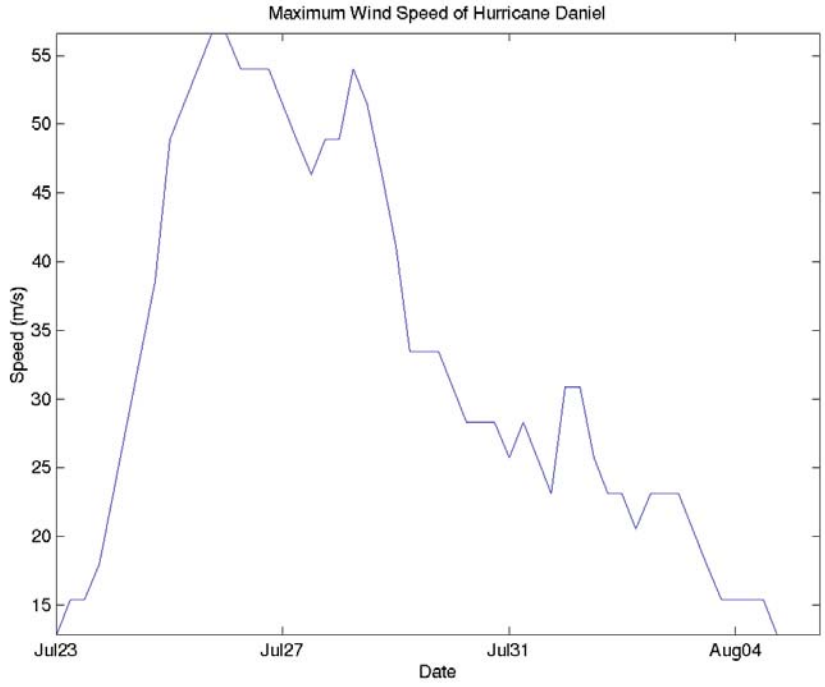

Figure 5. Track speed and maximum wind speed for Daniel.

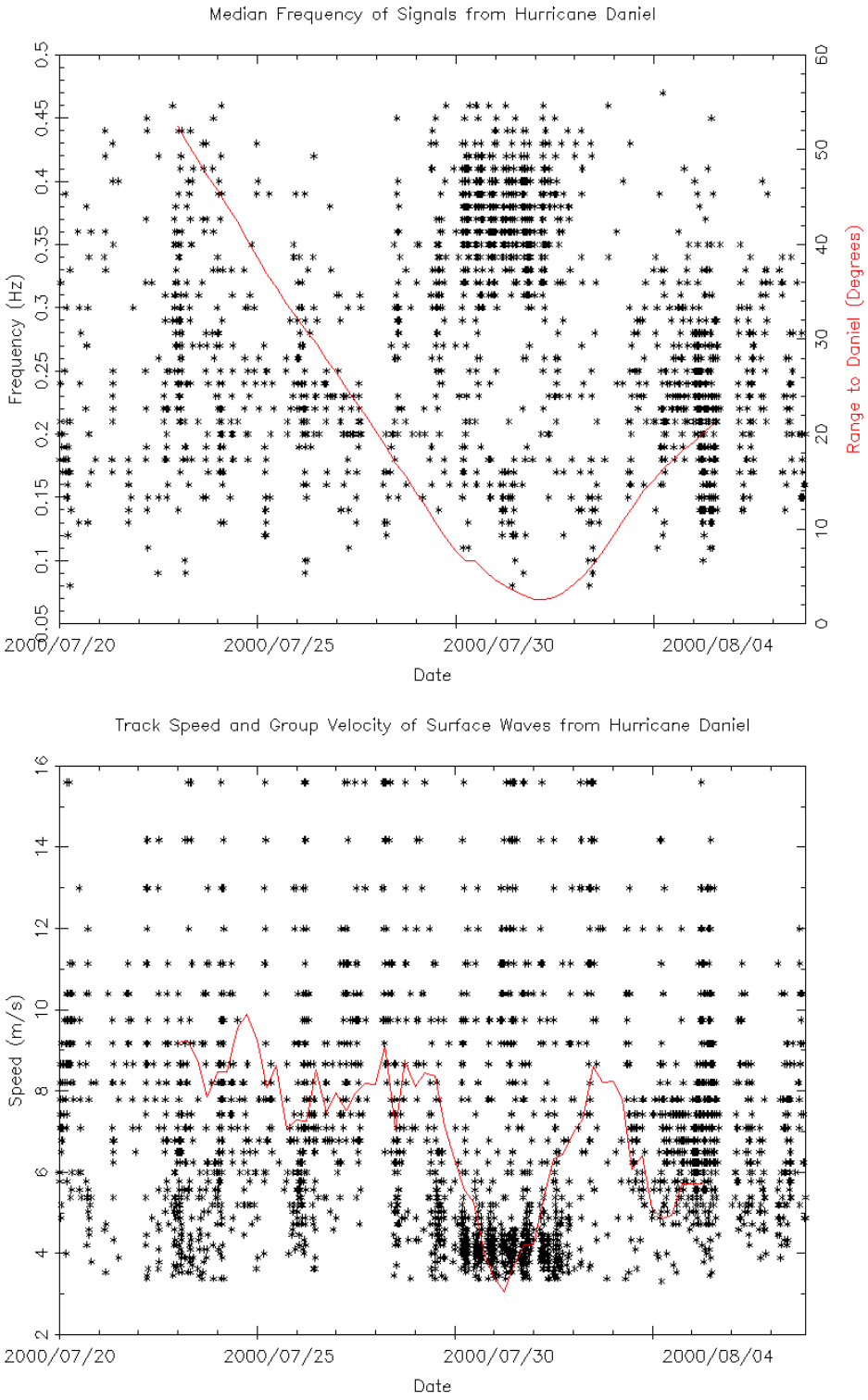

Figure 6. The upper panel shows the median frequency of peak detection and the range from KONA to the core of Daniel, and the lower panel shows Daniel's track speed (as in Figure 4) and the group velocity of surface waves corresponding to the acoustic median frequency. The track speed of Daniel exceeded the mean group velocity of the ocean waves up to the end of July 30, when Daniel is sufficiently close to Hawaii. From July 31-August 2, higher-frequency energy dominates, possibly due to the closer proximity of Daniel and the reflection of ocean waves from the island chain.